Coupling-Constant Dependence of Atomization Energies

MATTHIAS ERNZERHOF,[1] JOHN P. PERDEW,[1] KIERON BURKE[2]

[1] *Department of Physics and Quantum and Theory Group, Tulane University, New Orleans, Louisiana 70118*

[2] *Department of Chemistry, Rutgers University, Camden, New Jersey 08102*

Received 11 June 1996; revised 15 November 1996; accepted 25 November 1996

ABSTRACT: The local spin-density (LSD) functional and Perdew–Wang 91 (PW91) generalized gradient approximations to atomization energies of molecules are investigated. We discuss the coupling-constant dependence of the atomization energy and why exchange errors of the functionals are greater than exchange–correlation errors. This fact helps to justify hybrid schemes which mix some exact exchange with density functional approximations for exchange and correlation. It is shown that the biggest errors in the atomization energies occur when there is a strong interaction between different electron pairs, which vanishes upon atomization. We argue that the amount of exchange character of a molecular property, such as the atomization energy, depends on the property itself. We define an exact mixing coefficient b, which measures this exchange character, and show that both LSD and PW91 typically overestimate this quantity. Thus, nonempirical hybrid schemes which approximate this quantity by its LSD or PW91 value typically do not improve the exchange–correlation energy. Int J Quant Chem **64**: 285–295, 1997

I. Introduction

The development of generalized gradient approximations (GGAs) [1–7] has significantly extended the range of systems where density functional theory (DFT) can make useful predictions. Gradient-corrected density functionals are now routinely applied to quantum chemical problems. DFT is a relatively new means to investigate the molecular bond and, as with every other approach, leads to a new view of this fundamental problem. We focus on the coupling-constant decomposition [8, 9] of the atomization energy and explain how currently available density functional approximations produce useful predictions for the exchange–correlation contribution, ΔE_{xc}, which is typically greater than 50% of the total atomization energy.

Correspondence to: M. Ernzerhof.
Contract grant sponsor: Deutsche Forschungsgemeinschaft.
Contract grant sponsor: National Science Foundation.
Contract grant number: DMR95-21353.

 CCC 0020-7608 / 97 / 030285-11

In Section II, we introduce our notation and review the coupling-constant integration formula [8, 9]. The coupling-constant integral is used to derive a hybrid formula for the exchange–correlation energy in terms of the exchange energy and the exchange–correlation energy at full coupling strength in Section III. In Section IV, we investigate both the exchange and the coupling-constant averaged (exchange–correlation) contributions to atomization energies. In Section V, a modification of the hybrid formula of Section III is applied to atomization energies of molecules.

II. Coupling-Constant Integration

The ground-state energy of a (nonrelativistic) many-electron system may be written as

$$E = T + V_{ee} + V_{ext}, \tag{1}$$

where T is the interacting kinetic energy, V_{ee} is the expectation value of the Coulomb repulsion between electrons, and V_{ext} is the expectation value of the external potential. In Kohn–Sham density functional theory [10], Eq. (1) is rewritten in terms of a noninteracting reference wave function (the Kohn–Sham determinant), so that

$$E = T_s + U + V_{ext} + E_{xc}. \tag{2}$$

T_s denotes the kinetic energy of a noninteracting ground-state wave function which yields the exact density $\rho(\mathbf{r})$ of the interacting system and minimizes the kinetic energy. $U = \frac{1}{2}\int d^3r\, d^3r'\, \rho(\mathbf{r})\rho(\mathbf{r}')/|\mathbf{r}-\mathbf{r}'|$ is the classical or Hartree energy, and E_{xc} is the exchange–correlation energy, defined by Eqs. (1) and (2),

$$E_{xc} = V_{ee} - U + T_c. \tag{3}$$

$T_c = T - T_s$ is the difference between the interacting and noninteracting kinetic energies. The kinetic energy contribution to the exchange–correlation energy can be accounted for by a coupling-constant integration over purely potential contributions. Since the coupling-constant integration is one of our main concerns in the present work, we briefly review this formal procedure.

We define a coupling-constant dependent Hamiltonian

$$\hat{H}_\lambda = \hat{T} + \hat{V}_\lambda + \lambda \hat{V}_{ee}, \tag{4}$$

where $\hat{V}_\lambda = \int d^3r\, v_\lambda(\mathbf{r})\hat{\rho}(\mathbf{r})$ and the electron–electron repulsion operator $\hat{V}_{ee}$ is multiplied by the coupling-constant λ. The external potential v_λ, which is equal to the Kohn–Sham potential for $\lambda = 0$ and equal to v_{ext} for $\lambda = 1$, is adjusted to keep the density fixed and equal to the physical density for all values of λ. The ground-state energy of $\hat{H}_\lambda$ is denoted E_λ. Obviously

$$E = E_{\lambda=1} = E_{\lambda=0} + \int_o^1 d\lambda\, \frac{dE_\lambda}{d\lambda}. \tag{5}$$

From the Hellmann–Feynman theorem, $dE/d\lambda = \langle \psi_\lambda | \partial \hat{H}_\lambda / \partial\lambda | \psi_\lambda \rangle$ where ψ_λ is the ground-state wave function of $\hat{H}_\lambda$, we find [8, 9]

$$\frac{dE_\lambda}{d\lambda} = V_{ee,\lambda} + \int d^3r\, \rho(\mathbf{r}) \frac{dv_\lambda}{d\lambda} \tag{6}$$

where $V_{ee,\lambda} = \langle \psi_\lambda | \hat{V}_{ee} | \psi_\lambda \rangle$. From Eq. (4) we have

$$E_{\lambda=0} = T_s + \int d^3r\, \rho(\mathbf{r}) v_{\lambda=0}(\mathbf{r}). \tag{7}$$

Combining Eqs. (5), (6), and (7), we find

$$E = T_s + \int d^3r\, \rho(\mathbf{r}) v(\mathbf{r}) + \int_0^1 d\lambda\, V_{ee,\lambda}. \tag{8}$$

$V_{ee,\lambda}$ is usually decomposed into a λ-independent Hartree term U and the λ-dependent exchange–correlation energy $E_{xc,\lambda}$:

$$V_{ee,\lambda} = U + E_{xc,\lambda}. \tag{9}$$

We finally obtain

$$E = T_s + \int d^3r\, \rho(\mathbf{r}) v(\mathbf{r}) + U + \int_0^1 d\lambda\, E_{xc,\lambda}, \tag{10}$$

where the last integral is E_{xc}. This important result shows that the kinetic energy contribution to the correlation energy can be deduced from the λ dependence of $E_{xc,\lambda}$. Furthermore, this λ dependence can be extracted from the exchange–correlation energy functional via the exact scaling relation [11–13]

$$E_{xc,\lambda}[\,\rho] = \frac{d}{d\lambda}\left(\lambda^2 E_{xc}\left[\frac{\rho(\mathbf{r}/\lambda)}{\lambda^3}\right]\right). \tag{11}$$

To illustrate the nature of the λ dependence of $E_{xc,\lambda}$, in Figures 1 and 2 we show the coupling-constant dependence of $E_{xc,\lambda}/N$ for the homogeneous electron gas, as parametrized by Perdew

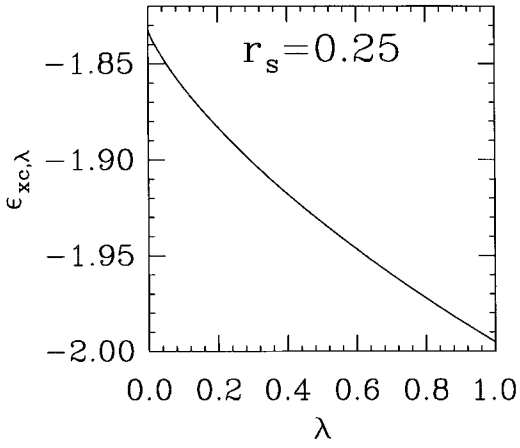

FIGURE 1. The λ-dependent exchange–correlation energy per particle of a uniform electron gas at a high density, $r_s = 0.25$ bohr, typical of core electrons (energy in hartrees).

and Wang [14]. This is the only system for which this dependence is known for all λ. We consider two electron densities characterized by the Seitz radius $r_s = (3/4\pi\rho)^{1/3}$. The first, $r_s = 0.25$, is a typical density of core electrons in an atom or molecule; note how nearly linear the curve in Figure 1 is. The second, $r_s = 6$, is typical of valence electrons in a low-density metal; note how much curvature develops in Figure 2.

More generally, under uniform scaling

$$\rho_\alpha(\mathbf{r}) = \alpha^3\rho(\alpha\mathbf{r}) \tag{12}$$

for any finite system, the λ-dependent curve becomes linear in the high-density ($\alpha \to \infty$) limit. On the other hand, as $\alpha \to 0$ in the low-density limit, the initial ($\lambda \to 0$) slope of the curve tends to $-\infty$, and the curve drops infinitely rapidly and becomes an α-dependent constant for all $\lambda > 0$.

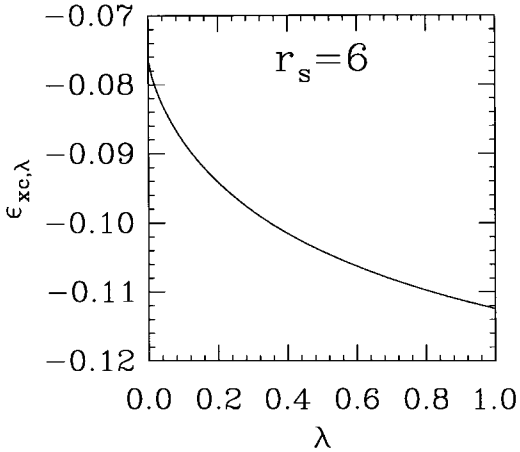

FIGURE 2. Same as Figure 1, but at a low density, $r_s = 6$ bohrs, typical of valence electrons.

For purposes of discussion, we will also need the exchange–correlation hole [15, 16] density $\rho_{xc}(\mathbf{r}, \mathbf{r}')$ around an electron at $\mathbf{r}$, which is itself a coupling-constant average,

$$\rho_{xc}(\mathbf{r}, \mathbf{r}') = \int_0^1 d\lambda\, \rho_{xc,\lambda}(\mathbf{r}, \mathbf{r}'),$$
$$\rho_{xc,\lambda}(\mathbf{r}, \mathbf{r}') = \{P_\lambda(\mathbf{r}, \mathbf{r}') - \rho(\mathbf{r})\rho(\mathbf{r}')\}/\rho(\mathbf{r}), \tag{13}$$

where $P_\lambda(\mathbf{r}, \mathbf{r}')$ is the pair density of ψ_λ,

$$P_\lambda(\mathbf{r}, \mathbf{r}') = N(N-1)\int d^3r_3 \ldots d^3r_N\, d\sigma_1 \ldots d\sigma_N \times \psi_\lambda^*(\mathbf{r}, \sigma_1, \mathbf{r}', \sigma_2, \mathbf{r}_3, \sigma_3, \ldots, \mathbf{r}_N, \sigma_N) \times \psi_\lambda(\mathbf{r}, \sigma_1, \mathbf{r}', \sigma_2, \mathbf{r}_3, \sigma_3, \ldots, \mathbf{r}_N, \sigma_N). \tag{14}$$

E_{xc} is given in terms of the exchange–correlation hole by

$$E_{xc} = \frac{1}{2}\int d^3r\, \rho(\mathbf{r}) \int d^3\mathbf{r}'\, \rho_{xc}(\mathbf{r}, \mathbf{r}')/|\mathbf{r}' - \mathbf{r}|. \tag{15}$$

The exchange–correlation hole fulfills the normalization condition [9],

$$\int d^3r'\, \rho_{xc}(\mathbf{r}, \mathbf{r}') = -1. \tag{16}$$

III. An Exact Mixing Coefficient

In this section, we define an exact exchange mixing coefficient [17–19], which tells us how much exchange to mix with $E_{xc,\lambda=1}$ to recover the exact exchange–correlation energy.

We use the mean value theorem to replace the coupling-constant integral $E_{xc} = \int_0^1 d\lambda\, E_{xc,\lambda}$ by a weighted sum of the integrand $E_{xc,\lambda}$ at the end points of the integration. Note that $E_{xc,\lambda}$ always lies below E_x, since correlation is always negative [20]. Since E_{xc} is an average over a monotonic curve beginning at E_x and ending at $E_{xc,\lambda=1}$, we can always find a number $0 \le b \le 1$ which satisfies

$$E_{xc} = bE_x + (1-b)E_{xc,\lambda=1}. \tag{17}$$

Solving for b, we find [21]

$$b = \frac{E_{\mathrm{xc}} - E_{\mathrm{xc},\,\lambda=1}}{E_x - E_{\mathrm{xc},\,\lambda=1}} = \frac{E_{c,\,\lambda=1} - E_c}{E_{c,\,\lambda=1}} = -\frac{T_c}{E_{c,\,\lambda=1}}. \tag{18}$$

From Eq. (17), we see that b is a coefficient which indicates how much exchange must be mixed with $E_{\mathrm{xc},\,\lambda=1}$ to recover E_{xc}. Since all the energies in Eq. (17) are functionals of the density, so too is b.

We may also interpret the inverse of b as a measure of the curvature of the λ-dependent curve, $E_{\mathrm{xc},\,\lambda}$. To see this, note that in the high-density limit (where $E_{\mathrm{xc},\,\lambda}$ is a straight line),

$$b[\,\rho_\alpha] \to \tfrac{1}{2}, \qquad \alpha \to \infty, \tag{19}$$

while in the low-density (or strong coupling) limit,

$$b[\,\rho_\alpha] \to 0, \qquad \alpha \to 0. \tag{20}$$

In fact, if E_{xc} is closer to $E_{\mathrm{xc},\,\lambda=1}$ than to E_x, as it is in all cases we are aware of, then the $E_{\mathrm{xc},\,\lambda}$ curve is concave upward, and $0 \le b \le \frac{1}{2}$. For the curves shown in Figures 1 and 2, we find $b(r_s = 0.25) = 0.42$ and $b(r_s = 6) = 0.29$, respectively. Thus the inverse of b measures the curvature, which in turn indicates the relative strength of correlation versus exchange in the system. For exchange-dominated systems, b is close to $\frac{1}{2}$; for strongly correlated systems, b is much lower. We will interpret b as the ''exchange character'' [17].

To finish this section, we discuss examples of b from quantum chemistry. Consider a system for which second-order perturbation theory (MP2) gives nearly the exact correlation energy, e.g., the Ne atom. In that case, $E_{\mathrm{xc},\,\lambda}$ is almost linear in λ, and b is close to $\frac{1}{2}$. On the other hand, if there is a near degeneracy of the Hartree–Fock determinant with excited determinants, then high-order perturbation expansions are necessary to obtain useful results. In such a system, the wave function changes very rapidly on going from zero to nonzero λ values, and rapidly approaches its $\lambda = 1$ value with increasing λ. An example is stretched H_2 [21–23], where for small but finite λ the wave function assumes its final ($\lambda = 1$) value and b is close to zero.

IV. Atomization Energies at $\lambda = 0$

In this section we discuss the exchange ($\lambda = 0$) energy contribution to the atomization energy of molecules. This means that we replace $\int_0^1 d\lambda\, E_{\mathrm{xc},\,\lambda}$ by $\int_0^1 d\lambda\, E_{\mathrm{xc},\,\lambda=0} = E_x$. We consider both the local spin-density (LSD) and the PW91 approximation to E_x. Self-consistent LSD calculations [24] have been performed and the exchange energy in the density functional approximations has been evaluated on the LSD densities. The exact exchange results ΔE_x are obtained by inserting the LSD Kohn–Sham orbitals into the Fock integral, which yields the exchange energy of a Slater determinant. Details of the calculation are given in the Appendix.

LSD APPROXIMATION

The formation of a covalent bond is accompanied by a compression of the molecular density, which also becomes more homogeneous than in the separated atoms [25]. This compression makes the exchange energy more negative at the LSD level of approximation. Because LSD overly favors density homogeneity, it therefore overbinds. The LSD decrease in exchange energy upon molecule formation is in general much too large, as can be seen by comparing ΔE_x with $\Delta E_x^{\mathrm{LSD}}$ in Table I. Note that the error in $\Delta E_x^{\mathrm{LSD}}$ is particularly big in cases where bond formation leads to electron pairs which strongly interact with each other (collected in the lower part of the table), i.e., electron pairs which are close to each other as in first-row multiple-bonded systems and in F_2. It is well known that F_2, although formally single-bonded, has strongly interacting lone pairs. In fact this interaction between the lone pairs is the reason the F_2 molecule is not stable in the Hartree–Fock approximation. On the other hand, the overlap between electron pairs leads to an increase in the electron density, which in turn causes an exaggerated decrease in the LSD exchange energy of the molecule.

In general, as shown in Table I, the exchange energy of the molecule is better described within the LSD approximation than the exchange energy of the separated atoms. We can understand this behavior in terms of the exchange hole. In the midbond region of a molecule, the two nuclei compete for the electron density and the exact

TABLE I
E_x^{LSD} contribution to atomization energies (D_e).[a]

System	ΔE_{xc} exact	E_x molecule	E_x atoms	ΔE_x exact	E_x^{LSD} molecule	E_x^{LSD} atoms	ΔE_x^{LSD}
H_2	0.090	−0.648	−0.597	0.051	−0.559	−0.513	0.045
LiH	0.080	−2.099	−2.059	0.041	−1.819	−1.779	0.040
CH_4	0.468	−6.536	−6.215	0.320	−5.864	−5.476	0.388
NH_3	0.328	−7.612	−7.440	0.171	−6.886	−6.627	0.259
OH	0.114	−8.489	−8.437	0.052	−7.685	−7.588	0.097
H_2O	0.262	−8.876	−8.736	0.140	−8.075	−7.845	0.231
HF	0.160	−10.343	−10.253	0.090	−9.438	−9.286	0.152
Li_2	0.035	−3.519	−3.520	−0.001	−3.049	−3.044	0.005
Cl_2	0.085	−54.909	−54.888	0.021	−50.746	−50.648	0.098
P_2	0.079	−45.055	−45.117	−0.062	−41.534	−41.488	0.046
$\bar{\delta}$	—	—	—	—	1.243	1.297	0.055
CO	0.213	−13.229	−13.159	0.070	−11.998	−11.780	0.217
N_2	0.137	−13.035	−13.088	−0.053	−11.824	−11.715	0.109
NO	0.106	−14.616	−14.682	−0.066	−13.300	−13.189	0.112
O_2	0.099	−16.224	−16.277	−0.053	−14.805	−14.663	0.142
F_2	0.009	−19.810	−19.930	−0.120	−18.124	−18.072	0.052
$\bar{\delta}$	—	—	—	—	1.373	1.543	0.171

[a] $\Delta E_{xc} \equiv E_{xc}$(atoms) − E_{xc}(molecule). The table is divided between systems with weakly and strongly interacting electron pairs. Exact (E_x) and LSD (E_x^{LSD}) exchange energies are shown. $\bar{\delta}$ denotes the mean absolute error. All energies are given in hartree (1 hartree = 627.5 kcal / mol).

exchange hole becomes more isotropic and centered on the reference electron compared to the exact exchange hole in the valence density of the separated atoms. In an atom, the exact exchange hole in the valence density is displaced toward the nucleus. The LSD exchange hole, however, is always centered on its reference electron, with the deepest point at the position of this electron. The LSD approximation neglects the displacement of the hole completely and therefore introduces a differential error in the exchange energy. The LSD approximation to ΔE_x does not compare well with the exact ΔE_x. Note, however, that ΔE_x^{LSD} is a much better approximation to the exact exchange–correlation energy difference ΔE_{xc}. This is a consequence of the fact that the LSD exchange hole is centered around the reference electron. In an inhomogeneous system, this centering of the hole is more appropriate for the exchange–correlation hole than for the exchange hole. This observation suggests that it is in general not a promising route to approximate the exchange energy and the correlation energy separately by a local or semilocal density functional. Indeed, it has been suggested that local or semilocal density functionals for exchange also include an estimate of static correlation [17–19, 22, 23, 26–29]. The ''exact'' ΔE_{xc} in Table I is obtained by subtracting $\Delta(E^{LSD} - E_{xc}^{LSD})$ from the experimental atomization energies.

PW91 APPROXIMATION

Density gradients make the GGA exchange energy more negative [7]. The gradients in the separated atoms are usually bigger than the gradients in the molecule, where we find a region of zero gradient in the midbond region [25, 30]. Therefore gradient corrections to LSD lower the energy of the atoms more than the energy of the molecule. This leads to a reduction of the overbinding of the local approximation, as shown in Table II.

The PW91 gradient-corrected exchange functional shows a significant improvement over LSD. For the single-bonded systems with weakly interacting bonds, such as H_2O and CH_4, ΔE_x^{PW91} agrees nicely with the exact results. For multiple-bonded systems we also observe a significant improvement, but the remaining error is larger. We attribute this error to the interaction between electron pairs. For the multiple-bonded systems, the

TABLE II
E_x^{PW91} contribution to atomization energies (D_e).

System	E_x molecule	E_x atoms	ΔE_x exact	E_x^{PW91} molecule	E_x^{PW91} atoms	ΔE_x^{PW91}	ΔE_x^{LSD}
H_2	−0.648	−0.597	0.051	−0.641	−0.589	0.052	0.045
LiH	−2.099	−2.059	0.041	−2.086	−2.040	0.045	0.040
CH_4	−6.536	−6.215	0.320	−6.521	−6.185	0.336	0.388
NH_3	−7.612	−7.440	0.171	−7.629	−7.412	0.217	0.259
OH	−8.489	−8.437	0.052	−8.518	−8.438	0.080	0.097
H_2O	−8.876	−8.736	0.140	−8.919	−8.732	0.187	0.231
HF	−10.343	−10.253	0.090	−10.395	−10.271	0.124	0.152
Li_2	−3.519	−3.520	−0.001	−3.498	−3.492	0.007	0.005
Cl_2	−54.909	−54.888	0.021	−54.904	−54.849	0.056	0.098
P_2	−45.055	−45.117	−0.062	−45.084	−45.077	0.007	0.046
$\bar{\delta}$	—	—	—	0.023	0.022	0.029	0.055
CO	−13.229	−13.159	0.070	−13.309	−13.151	0.158	0.217
N_2	−13.035	−13.088	−0.053	−13.123	−13.058	0.065	0.109
NO	−14.616	−14.682	−0.066	−14.729	−14.672	0.057	0.112
O_2	−16.224	−16.277	−0.053	−16.361	−16.287	0.074	0.142
F_2	−19.810	−19.930	−0.120	−19.967	−19.963	0.003	0.052
$\bar{\delta}$	—	—	—	0.115	0.018	0.116	0.171

molecule is less accurately described by the GGA approximation than are the separated atoms. A plausible explanation is that the GGA exchange–correlation hole is off-center, but too localized around its electron, like the hole in an atom. For single-bonded systems, there is no clear pattern with regard to the question whether the molecule or the atom is better described.

To support our claim that the interaction between electron pairs gives rise to an additional error in the differential exchange energy for LSD and PW91, we consider the NH_3 molecule and compare the performance of the LSD and PW91 exchange functionals at the experimental geometry and at a distorted geometry, in which the H—N—H angle has been reduced to 51.3° from its experimental value of 106.7°. The N—H bond length is kept fixed. From Table III we see that the error in the PW91 exchange energy increases significantly if the binding electron pairs are pushed together. The decrease in exchange energy on squeezing the molecule is overestimated by a factor of 2 both in LSD and PW91. The magnitude of this error is comparable to the difference between the error in atomization energy of single- and multiple-bonded systems.

The presence of several different orbitals in the same region of space can give rise to complicated and highly delocalized exchange holes which are poorly described by local or semilocal density functional approximations. In particular, the effects of orbital nodality have been discussed by

TABLE III
Interaction between electron pairs in NH_3.

< (H—N—H)	E_x	E_x^{LSD}	LSD error	E_x^{PW91}	PW91 error
106.7°	−7.612	−6.886	0.726	−7.629	−0.017
51.3°	−7.626	−6.921	0.705	−7.658	−0.032
Change	−0.014	−0.034	−0.021	−0.029	−0.015

Gunnarsson and Jones [31]. Thus, while the density functional exchange energy always becomes more negative when the molecule is formed ($\Delta E_x^{\mathrm{DFT}} > 0$), the exact exchange energy sometimes becomes less negative ($\Delta E_x < 0$), as shown in Tables I and II.

COUPLING-CONSTANT AVERAGED ATOMIZATION ENERGIES

It is expected that density functional approximations to $E_{\mathrm{xc},\lambda}$ work better for large compared to small values of λ [17–19, 32]. The λ-average E_{xc} of $E_{\mathrm{xc},\lambda}$ is therefore in general better approximated than $E_x = E_{\mathrm{xc},\lambda=0}$.

Table IV shows that we indeed find a remarkable improvement in the density functional approximations to E_{xc} over the approximations to E_x. With increasing λ, the on-top value of the exchange–correlation hole becomes deeper, and the sum rule of Eq. (14) ensures that the hole becomes more short-ranged and centered around its reference electron, so that information about the local density and the gradient of the density is sufficient to model the hole very accurately. The general trend which emerges from Table IV is that atomization energies are overestimated by the approximate density functionals used in this work. This overestimation is greatly exaggerated at the exchange-only level. But the error made at the lower end of the coupling-constant integration is not uniform: it is big for multiple-bonded systems and small for single-bonded systems. This effect carries over (to a much smaller extent) to the coupling-constant averaged quantity E_{xc}, so that the atomization energy for multiple-bonded systems is less accurately reproduced than the atomization energy of single-bonded systems.

TABLE IV
Atomization energies (D_e) in the LSD and PW91 approximation.

System	$\Delta E^{\mathrm{exact}}$	ΔE^{LSD}	ΔE^{PW91}
H_2	0.1743	0.1799	0.1680
LiH	0.0921	0.0955	0.0850
CH_4	0.6682	0.7359	0.6721
NH_3	0.4740	0.5367	0.4831
OH	0.1697	0.1975	0.1761
H_2O	0.3700	0.4240	0.3755
HF	0.2243	0.2580	0.2279
Li_2	0.0389	0.0368	0.0326
Cl_2	0.0924	0.1281	0.1017
P_2	0.1869	0.2264	0.1917
$\bar{\delta}$	—	0.033	0.006
CO	0.4129	0.4763	0.4288
N_2	0.3643	0.4259	0.3864
NO	0.2437	0.3164	0.2731
O_2	0.1920	0.2785	0.2287
F_2	0.0614	0.1255	0.0875
$\bar{\delta}$	—	0.070	0.026

We now sketch the coupling-constant dependence of $\Delta E_{\mathrm{xc},\lambda} = E_{\mathrm{xc},\lambda}^{\mathrm{atoms}} - E_{\mathrm{xc},\lambda}^{\mathrm{molecule}}$ for the N_2 molecule in Figure 3. $\Delta E_{\mathrm{xc},\lambda}^{\mathrm{LSD}}$ and $\Delta E_{\mathrm{xc},\lambda}^{\mathrm{PW91}}$ are calculated using Eq. (11), while the ''exact'' curve is a sketch. In the separated atoms we do not have much static correlation, so $\Delta E_{\mathrm{xc},\lambda}$ can be accurately obtained from low-order perturbation theory, which implies that $E_{\mathrm{xc},\lambda}^{\mathrm{atoms}}$ is close to a straight line. The N_2 molecule shows strong static correlation. Static correlation causes $E_{\mathrm{xc},\lambda}^{\mathrm{molecule}}$ to drop more rapidly from its $\lambda = 0$ value toward its $\lambda = 1$ value. Based on these observations, we expect that the $\Delta E_{\mathrm{xc},\lambda}$ curve goes rapidly away from its exchange-only (i.e., $\lambda = 0$) value and then linearly approaches the $\lambda = 1$ value. The $\lambda = 1$ value of $\Delta E_{\mathrm{xc},\lambda}$ is drawn assuming it to be exactly reproduced in the PW91 approximation. The LSD curve overestimates $\Delta E_{\mathrm{xc},\lambda}$ at $\lambda = 1$, but its error is much smaller there than at the $\lambda = 0$ end. In cases where we have less static correlation (i.e., in single-bonded systems), the approximate density functional and exact curves match each other more closely and the difference at $\lambda = 0$ is much smaller. The qualitative picture of the λ dependence of $\Delta E_{\mathrm{xc},\lambda}$ given here has been confirmed by the suc-

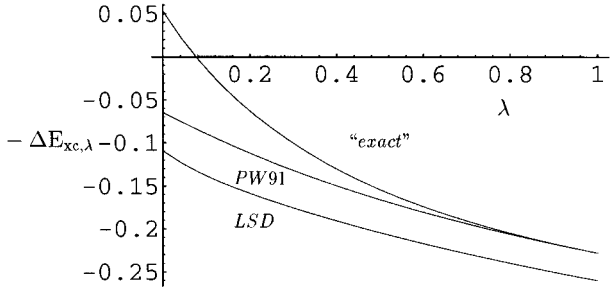

FIGURE 3. Sketch of $\Delta E_{\mathrm{xc},\lambda}$ for $N_2 \rightarrow 2N$ (energy in hartrees). Since we could not find an ''exact'' correlated wave function for N_2, we have constructed the ''exact'' curve to agree with PW91 at $\lambda = 1$.

cessful construction of nonempirical hybrid schemes [33–35] and by the calculation of the exact $dE_{\mathrm{xc},\lambda}/d\lambda|_{\lambda=0}$ [35].

V. Hybrids Based on the Mixing Coefficient

Now we use the LSD or PW91 approximation for $E_{c,\lambda}$ together with Eq. (18) to determine the mixing coefficient b, which is a measure of the exchange contribution to E_{xc}. This recipe ($b = b^{\mathrm{DFA}}$) ensures that b is exact in cases where the approximate density functional is exact, so that we recover the correct limit for slowly varying densities. Other choices which reproduce the exact b in the limit of slowly varying densities are also possible, but they require further information about the exchange character of the system of interest.

A simple prescription is to use a density functional approximation (DFA) for both $E_{\mathrm{xc},\lambda=1}$ and b in Eq. (17), and the exact exchange energy for E_x, which is less accurately approximated by density functionals. We evaluate the exact exchange energy by inserting the DFA Kohn–Sham orbitals into the Fock integral for the exchange energy of a Slater determinant. We obtain the hybrid energy

$$E_{\mathrm{xc}}^{\mathrm{hyb}} = b^{\mathrm{DFA}} E_x^{\mathrm{exact}} + (1 - b^{\mathrm{DFA}}) E_{\mathrm{xc},\lambda=1}^{\mathrm{DFA}}. \quad (21)$$

From Eq. (17) it follows that

$$E_c^{\mathrm{DFA}} = (1 - b^{\mathrm{DFA}}) E_{c,\lambda=1}^{\mathrm{DFA}}, \quad (22)$$

which, inserted into Eq. (21), leads to

$$\begin{aligned} E_{\mathrm{xc}}^{\mathrm{hyb}} &= b^{\mathrm{DFA}} E_x^{\mathrm{exact}} + (1 - b^{\mathrm{DFA}}) E_x^{\mathrm{DFA}} + E_c^{\mathrm{DFA}} \\ &= b^{\mathrm{DFA}} (E_x^{\mathrm{exact}} - E_x^{\mathrm{DFA}}) + E_{xc}^{\mathrm{DFA}}. \end{aligned} \quad (23)$$

Becke's recent empirical hybrid scheme [17] makes use of an expression similar to Eq. (23):

$$E_{\mathrm{xc}}^{\mathrm{empir}} = a(E_x^{\mathrm{exact}} - E_x^{\mathrm{DFA}}) + E_{\mathrm{xc}}^{\mathrm{DFA}}, \quad (24)$$

where the empirical parameter a is 0.16 or 0.28 [17] depending on the GGA used. Note that a in Eq. (24) is usually chosen to be the same constant for all systems. It does not have the same meaning as the parameter $b^{\mathrm{DFT}} = -T_c^{\mathrm{DFA}}/E_{c,\lambda=1}^{\mathrm{DFA}}$, which is system-dependent. In Eq. (21), b^{DFA} determines the amount of $E_{c,\lambda=1}^{\mathrm{DFA}}$ contributing to $E_{\mathrm{xc}}^{\mathrm{hyb}}$, and so, for the hybrid constructed here, can be considered as a nonempirical estimate of the value a. The empirical approach to determine a is based on fits to energy differences upon ionization, atomization, and proton attachment [17]. The empirically determined single value for a may be characteristic of the properties it is fitted to, just as b^{Δ} is, as argued below. A fit of a to a set of atomization and ionization energies and proton affinities may not be optimal for properties which are mainly determined by core electrons, or are otherwise different from those to which a was fitted. Note that Gritsenko, van Leeuwen, and Baerends [21] use Eq. (21) with $b^{\mathrm{DFA}} \rightarrow b^{\mathrm{exact}}$, where b^{exact} is determined for each system by Eq. (18).

In general, Eq. (23) needs to be modified if we want to calculate molecular properties such as atomization energies. This can be seen by the following argument: b^{DFA}, which measures the exchange contribution to E_{xc}^{hyb}, is in part determined by electrons which do not participate in the atomization process, e.g., core electrons. The high-density core electrons are well described by second-order perturbation theory, so that the more core electrons we have, the closer b will be to $\frac{1}{2}$ [as in Eq. (19)]. But $b = \frac{1}{2}$ is not appropriate for the valence electrons (see Fig. 2). We need to find a way to eliminate the contribution to the parameter b from electrons which do not participate in the atomization process.

To account for this property dependence of the amount of exchange mixing, we turn the above scheme for the calculation of $E_{\mathrm{xc}}^{\mathrm{hyb}}$ into a scheme for the calculation of energy differences and the corresponding b^{Δ}:

$$\Delta E_{\mathrm{xc}}^{\mathrm{hyb}} = b^{\Delta}(\Delta E_x^{\mathrm{exact}} - \Delta E_x^{\mathrm{DFA}}) + \Delta E_{\mathrm{xc}}^{\mathrm{DFA}}, \quad (25)$$

where

$$b^{\Delta} = -\frac{\Delta T_c^{\mathrm{DFA}}}{\Delta E_{c,\lambda=1}^{\mathrm{DFA}}}. \quad (26)$$

An alternative way to reduce the effect of the core electrons on the parameter b would be to use a pseudopotential. Note that in the energy-difference hybrid approach no attempt is made to define a unique energy for a given system.

A special case in which the above hybrid form becomes exact is when the shape of the exact λ-dependent curve follows precisely that of the DFA curve, being identical at $\lambda = 1$ but differing

at $\lambda = 0$, i.e., when

$$\frac{E_{xc,\lambda} - E_{xc,\lambda=1}}{E_{xc,\lambda}^{DFA} - E_{xc,\lambda=1}^{DFA}} = \text{constant} \qquad (27)$$

(or a similar equation for energy differences). Under these circumstances, $b^{DFA} = b$, and the hybrid of Eq. (21) reproduces the exact exchange–correlation energy. Unfortunately, as can be seen from Figure 3, the fact that the exchange error of the approximate functionals is far greater than the exchange–correlation error suggests that Eq. (27) is not valid for atomization energies. The following tables, giving results based on this hybrid, also suggest that this assumption is incorrect.

First we discuss the results obtained by using the LSD approximation in the energy difference hybrid. Table V compares the LSD approximation to the atomization energies of a number of small atoms with the results obtained from the energy-difference hybrid. We see that the energy difference hybrid gives an improvement compared to the LSD approximation. Note, however, that Becke has shown [19] that even the extreme value $b = 0.5$ leads to significant improvements over LSD. Therefore any mixing coefficient $0 \le b \le 0.5$ gives an overall improvement of the atomization energies, since atomization energies at the LSD level are always too high and the atomization energies at the Hartree–Fock level are always too low. As already mentioned, the choice of $b = 0.5$ is consistent with the assumption that second-order perturbation theory gives the correct atomization energy. Results obtained with this half-and-half approach (i.e., $b = 0.5$) are also listed in Table V; they tend to overcorrect the LSD atomization energies in some cases. Note also that the mixing coefficients given in Table V do not reflect expectations about the Hartree–Fock character of the molecules. We would expect the CH_4 molecule to have more Hartree–Fock character than the N_2 molecule. We conclude that the energy difference hybrid in the LSD approximation shows an error cancellation which results in good predictions for the atomization energies. Because $\Delta E_{xc,\lambda=1}^{LSD}$ is much larger than $\Delta E_{xc,\lambda=1}$ (as shown in Fig. 3), an excessive ($b = \frac{1}{2}$) mixing of exact exchange accidentally cancels this $\lambda = 1$ error of LSD.

We can also use the PW91 approximation for the exchange and correlation energy functionals in Eq. (23). The results for atomization energies from this hybrid scheme are reported in Table VI. We

TABLE V

E_{xc} contribution to the atomization energies (D_e) from hybrid schemes based on the LSD approximation. "h & h" is the half-and-half hybrid ($b = 1/2$).

System	ΔE_{xc}	ΔE_{xc}^{LSD}	$\Delta E_{xc}^{h\&h}$	ΔE_{xc}^{Δ}	b^{Δ}
H_2	0.090	0.096	0.088	0.098	0.365
LiH	0.080	0.083	0.074	0.084	0.353
CH_4	0.468	0.535	0.473	0.510	0.382
NH_3	0.328	0.391	0.322	0.357	0.385
OH	0.114	0.142	0.111	0.125	0.389
H_2O	0.262	0.316	0.256	0.281	0.389
HF	0.160	0.194	0.156	0.170	0.392
Li_2	0.035	0.033	0.022	0.031	0.313
Cl_2	0.085	0.121	0.078	0.089	0.410
P_2	0.079	0.119	0.051	0.077	0.381
$\bar{\delta}$	—	0.033	0.008	0.013	—
CO	0.213	0.276	0.194	0.216	0.410
N_2	0.137	0.199	0.103	0.133	0.403
NO	0.106	0.178	0.079	0.106	0.406
O_2	0.099	0.186	0.082	0.105	0.413
F_2	0.009	0.074	−0.016	0.002	0.417
$\bar{\delta}$	—	0.070	0.024	0.004	—

TABLE VI

E_{xc} contribution to the atomization energies (D_e) from hybrid schemes based on the PW91 approximation.

System	ΔE_{xc}	ΔE_{xc}^{PW91}	$\Delta E_{xc}^{h\&h}$	ΔE_{xc}^{Δ}	b^{Δ}
H_2	0.090	0.084	0.079	0.084	0.424
LiH	0.080	0.073	0.067	0.071	0.423
CH_4	0.468	0.472	0.443	0.465	0.412
NH_3	0.328	0.337	0.297	0.318	0.417
OH	0.114	0.121	0.101	0.109	0.423
H_2O	0.262	0.268	0.233	0.248	0.421
HF	0.160	0.164	0.142	0.150	0.426
Li_2	0.035	0.028	0.020	0.026	0.359
Cl_2	0.085	0.094	0.070	0.081	0.389
P_2	0.079	0.084	0.036	0.057	0.394
$\bar{\delta}$	—	0.006	0.021	0.009	—
CO	0.213	0.229	0.175	0.192	0.418
N_2	0.137	0.159	0.087	0.110	0.418
NO	0.106	0.135	0.062	0.084	0.416
O_2	0.099	0.136	0.063	0.084	0.412
F_2	0.009	0.036	−0.031	−0.017	0.423
$\bar{\delta}$	—	0.026	0.042	0.022	—

do not obtain a consistent improvement over PW91. To understand why, note that the sketch Figure 3 shows that $\Delta E_{\mathrm{xc},\lambda}^{\mathrm{PW91}}$ has too little curvature, so that b, which measures the inverse curvature, is overestimated.

For completeness, we also report results for the half-and-half approach. In both hybrids we obtain a large overcorrection. At the more accurate PW91 level we therefore see that $b = \frac{1}{2}$ is quite unrealistic. Note that the mixing coefficient b^{PW91} agrees better than b^{LSD} with our expectation about the Hartree–Fock character of the atomization processes of the various molecules.

VI. Conclusion

The coupling-constant analysis shows that the major error made in the LSD and PW91 calculation of atomization energies comes from the lower end of the coupling-constant integration. Furthermore, the exchange contribution to atomization energies is badly approximated in cases where we have strong static correlation effects in the molecule, including first-row multiple-bonded systems with many interacting electron pairs. The local and semilocal density functional approximations studied here are derived from the homogeneous or slowly varying electron gas and are not expected to describe finite systems with strong static correlation as accurately as systems with dynamic correlation. Based on our sketch for the coupling-constant dependence of $\Delta E_{\mathrm{xc},\lambda}$, we see that the λ dependence predicted by the density functionals is much closer to a straight line than is the exact $\Delta E_{\mathrm{xc},\lambda}$. This helps, however, to reduce the error in $\Delta E_{\mathrm{xc}}^{\mathrm{LSD/PW91}}$: while ΔE_x is overestimated by approximate density functionals, ΔE_c is underestimated. The fact that $\Delta E_{\mathrm{xc},\lambda}^{\mathrm{PW91}}$ is too straight implies that the mixing coefficient which we obtain from $b^{\Delta} = -\Delta T_c/\Delta E_{\mathrm{xc},\lambda=1}$, with PW91 input, is too big. A simple hybrid scheme using this b^{Δ} therefore tends to overcorrect the overbinding tendency of the PW91 approximation. We conclude that the successful construction of a nonempirical hybrid requires further insight into the coupling-constant dependence of $\Delta E_{\mathrm{xc},\lambda}$. After this article was completed, work on this question led to nonempirical hybrid schemes [33–35], which verify the discussion of the adiabatic connection presented here.

Appendix: Technical Details of the Calculations

The calculations reported in this work are performed with a modified version of the CADPAC program [24]. The electron densities are obtained from unrestricted Kohn–Sham calculations in the LSD approximation, and the various functionals have been evaluated on these densities. Nonspherical densities and Kohn–Sham potentials have been used for open-shell atoms [36]. The experimental geometries employed in our work are listed in Ref. [37]. The D_e values are obtained from the experimental atomization energies and the zero point energies given in Ref. [38]. The Gaussian basis sets used are of triple zeta quality with up to $l + 2$-type polarization functions for H and for the first-row elements and $l + 1$-type polarization functions for the second-row elements. l is the angular momentum number of the highest occupied orbital in the atom.

ACKNOWLEDGMENTS

This work was supported in part by the Deutsche Forschungsgemeinschaft, and in part by the National Science Foundation under grant DMR95-21353. We thank Jan Baerends for a preprint of Ref. [21].

References

1. D. C. Langreth and M. J. Mehl, Phys. Rev. B **28**, 1809 (1983).
2. J. P. Perdew, Phys. Rev. B **33**, 8822 (1986).
3. J. P. Perdew and Y. Wang, Phys. Rev. B **33**, 8800 (1986).
4. A. D. Becke, Phys, Rev. A **38**, 3098 (1988).
5. C. Lee, W. Yang, and R. G. Parr, Phys. Rev. B **37**, 785 (1988).
6. J. P. Perdew, in *Electronic Structure of Solids 91*, P. Ziesche and H. Eschrig, Eds. (Akademie Verlag, Berlin, 1991).
7. J. P. Perdew, J. A. Chevary, S. H. Vosko, K. A. Jackson, M. R. Pederson, D. J. Singh, and C. Fiolhais, Phys. Rev. B **46**, 6671 (1992); **48**, 4978 (1993) (E).
8. D. C. Langreth and J. P. Perdew, Solid State Comm. **17**, 1425 (1975).
9. R. G. Parr and W. Yang, *Density-Functional Theory of Atoms and Molecules* (Oxford University Press, Oxford, 1989); R. M. Dreizler and E. K. U. Gross, *Density Functional Theory* (Springer Verlag, Berlin, 1990).
10. W. Kohn and L. J. Sham, Phys. Rev. A **140**, 1133 (1965).
11. M. Levy and J. P. Perdew, Phys. Rev. A **33**, 2010 (1985).
12. M. Levy, N. H. March, and N. C. Handy, J. Chem. Phys. **104**, 1989 (1996).

13. A. Görling and M. Levy, Phys. Rev. B **47**, 13105 (1993).
14. J. P. Perdew and Y. Wang, Phys. Rev. B **45**, 13244 (1992).
15. K. Burke, J. P. Perdew, and M. Ernzerhof, in preparation.
16. O. Gunnarson and B. I. Lundqvist, Phys. Rev. B **13**, 4274 (1976).
17. A. D. Becke, J. Chem. Phys. **104**, 1040 (1996).
18. A. D. Becke, J. Chem. Phys. **98**, 5648 (1993).
19. A. D. Becke, J. Chem. Phys. **98**, 1372 (1993).
20. M. Levy, Phys. Rev. A **43**, 4637 (1991).
21. O. Gritsenko, R. van Leeuwen, and E. J. Baerends, Int. J. Quant. Chem., to appear. During the preparation of this manuscript, we received this preprint in which Eq. (18) has been derived independently.
22. J. P. Perdew, A. Savin, and K. Burke, Phys. Rev. A **51**, 4531 (1995).
23. J. P. Perdew, M. Ernzerhof, K. Burke, and A. Savin, Int. J. Quant. Chem. **61**, 197 (1997).
24. CADPAC6: The Cambridge Analytical Derivatives Package Issue 6.0 Cambridge (1995). A suite for quantum chemistry programs developed by R. D. Amos, I. L. Alberts, J. S. Andrews, S. M. Colwell, N. C. Handy, D. Jayatilaka, P. J. Knowles, R. Kobayashi, G. J. Laming, A. M. Lee, P. E. Maslen, C. W. Murray, P. Palmieri, J. E. Rice, J. Sanz, E. D. Simandiras, A. J. Stone, M.-D. Su, and D. J. Tozer.
25. A. Zupan, K. Burke, M. Ernzerhof, and J. P. Perdew, J. Chem. Phys., submitted.
26. J. C. Slater and K. H. Johnson, Phys. Rev. B **5**, 844 (1971).
27. M. Cook and M. Karplus, J. Phys. Chem. **91**, 31 (1987).
28. V. Tschinke and T. Ziegler, J. Chem. Phys. **93**, 8051 (1990).
29. R. Neumann, R. Nobes, and N. Handy, Mol. Phys. **87**, 1 (1996).
30. R. van Leeuwen and E. Baerends, Int. J. Quant. Chem. **52**, 711 (1994).
31. O. Gunnarson and R. O. Jones, Phys. Rev. B **31**, 7588 (1985).
32. M. Ernzerhof, J. P. Perdew, and K. Burke, in *Density Functional Theory*, R. Nalewajski, Ed. (Springer-Verlag, Berlin, 1996).
33. J. P. Perdew, M. Ernzerhof, and K. Burke, J. Chem. Phys. **105**, 9982 (1996).
34. K. Burke, M. Ernzerhof, and J. P. Perdew, Chem. Phys. Lett., to appear.
35. M. Ernzerhof, Chem. Phys. Lett. **263**, 499 (1996).
36. F. W. Kutzler and G. S. Painter, Phys. Rev. Lett. **59**, 1285 (1987).
37. D. J. DeFrees, B. A. Levi, S. K. Pollack, W. J. Hehre, J. S. Binkley, and J. A. Pople, J. Am. Chem. Soc. **101**(**15**), 4085 (1979). Geometries of NO, Cl_2 and P_2 are from K. P. Huber and G. Herzberg, *Molecular Spectra and Molecular Structure IV: Constants of Diatomic Molecules* (Van Nostrand Reinhold, New York, 1979).
38. J. A. Pople, M. Head-Gordon, D. J. Fox, K. Raghavachari, L. A. Curtiss, J. Chem. Phys. **90**, 5622 (1989); L. A. Curtiss, C. Jones, G. W. Trucks, K. Raghavachari, and J. A. Pople, J. Chem. Phys. **93**, 2537 (1990).